VERTEBRATE ZOOLOGY

70 (1): 9–22
2020

SENCKENBERG

VIRTUAL ISSUE on Recent Advances in Chondrocranium Research | Guest Editor: Ingmar Werneburg

Knockdown of *zax* in *Xenopus laevis* leads to craniofacial malformations and the absence of the intramandibular joint

Paul Lukas*, Jennifer Schmidt, Lennart Olsson

Institut für Zoologie und Evolutionsforschung mit Phyletischem Museum, Ernst-Haeckel-Haus und Biologiedidaktik — * Corresponding author: paul.lukas@uni-jena.de

Submitted August 22, 2019.
Accepted October 4, 2019.
Published online at www.senckenberg.de/vertebrate-zoology on October 21, 2019.
Published in print Q1/2020.

Editor in charge: Ingmar Werneburg

Abstract

The jaws of anuran tadpoles consist of several evolutionary novelties, which are unique within the vertebrates. The most noticeable of these novelties are two cartilaginous elements called rostralia and the derived organisation of cranial muscles, which form an entirely new feeding apparatus. The suprarostral cartilage is located in the upper and the infrarostral cartilages in the lower jaw. Between infrarostral and Meckel's cartilage an intramandibular joint is present. The morphological diversity of anuran tadpoles and their different feeding modes could be associated with these cartilaginous innovations and the shifted insertions of various cranial muscles. The evolutionary origin of the rostralia and, more generally, of evolutionary novelties remains unclear most widely. Therefore, we investigated the molecular basis of the morphogenesis of the infrarostrals by functional knock-down of the bagpipe-related homeobox gene zampogna (*zax*) in *Xenopus laevis*. Its knockdown caused fatal deformation of the anterior part of the head and disappearance of the infrarostrals as well as shifted muscular insertions. Higher doses caused a total loss of head structures including mouth, eyes and cranial cartilages. Using quantitative PCR, we found a correlation between cartilage formation and the expression of *zax*. Our findings indicate that *zax* is part of a regulatory gene network controlling the development of the ventral part of the anuran head and the formation of the intramandibular joint. This supports the view that not the infrarostrals but rather the intramandibular joint, which forms in a *zax*-dependent manner, is the actual evolutionary novelty.

Key words

Bagpipe-related homeobox gene, morphogenesis, *nkx 3-3*, novelties, rostralia, *Xenopus laevis*.

Introduction

The evolution of upper and lower jaws in gnathostomes was an important innovation that enabled predation and handling of large and motile prey. The jaw itself consists of several ventral and dorsal elements connected by a distinct joint (Cerny *et al.*, 2010). The mouth region has undergone further changes in different gnathostome groups. One of the more spectacular is the presence of rostral cartilages and related changes to the pattern of cranial musculature in anuran tadpoles. A new feeding apparatus is produced, in which the suprarostral cartilage and the infrarostral cartilage are present (Fig. 1). The suprarostral cartilage belongs to the upper jaw and is movable against the chondrocranium. The infrarostral cartilage forms the anterior part of the lower jaw and is connected to Meckel's cartilage via the intramandibular joint (McDiarmid & Altig, 1999). This has facilitated the evolution of the numerous different feeding modes (filter feeding, rasping, carnivory etc.) seen in tadpoles. Furthermore, the larval stage is decoupled from the adult stage. The morphology as well as the underlying genetic background can evolve independently in anuran larvae and adults (Wollenberg Valero *et al.*, 2017). This fact

is often seen as the major reason why anurans are the dominant recent amphibian group both ecologically and in terms of diversity (Svensson & Haas, 2005).

Xenopus laevis (Daudin, 1802) belongs to the Pipidae a family of tongueless frogs. The tadpole of *X. laevis* is highly derived and shows pipoid-specific features (Fig. 1) such as a plate-like suprarostral, broad commissura quadratocranialis anterior, a reduced muscular process of the palatoquadrate and precocious formation of the larval lower jaw (De sá & swart, 1999). The suprarostral cartilage and its alae are fused to the cornua trabeculae and form a crescent-shaped, immobile suprarostral plate, which supports the tentacular cartilage in the upper jaw (De Sá & Swart, 1999, Rose *et al.*, 2015). In the lower jaw the infrarostrals are fused medially and articulate with Meckel's cartilage (Sokol, 1977). The muscular process of the palatoquadrate is reduced and a lateral process of the palatoquadrate is present (De Sá & Swart, 1999). The appearance of the rostralia in anurans required a repatterning of several cranial muscles. For example, the m. geniohyoideus inserts at the anterior tip of Meckel's cartilage in more basal lineages (Ziermann & Diogo, 2013) but on the infrarostral cartilages in *X. laevis* (Ziermann & Olsson, 2007).

Neural crest-derived cells are responsible for the formation of these novel cartilages (Olsson & Hanken, 1996; Gross & Hanken, 2008). The shape of neural crest-derived cartilages depends on the expression of homeobox genes in cranial neural crest progenitor cells before migration (Rose, 2009). This pattern defines the anterior-posterior-shape of the cartilages (Rose, 2009). Dorsoventral identity is defined by the expression of dlx genes (Beverdam *et al.*, 2002; Depew *et al.*, 2002). The evolutionary origin of these novel cartilages and the mechanisms, which gave rise to them are widely unknown. Svensson & Haas (2005) proposed three different ways for how new cartilages like the rostralia could have arisen during evolution. (I) The cartilage itself could be the novelty or (II) the result of a duplication event, or (III) the rostralia could be partitioned regions of pre-existing cartilages. Square *et al.* (2015) excluded de novo evolution of the infrarostral cartilage because it has a transcription factor expression profile similar to the ventralmost aspect of the first pharyngeal arch in gnathostomes lacking rostralia. Molecular evidence for a duplication event within the first pharyngeal arch could not be found either (Square *et al.*, 2015). If the cartilage is partitioned by several molecular signals the real novelties are not the cartilages itself but the articulations between Meckel's cartilage and the infrarostal and between the suprarostral and the chondrocranium (Svensson & Haas, 2005). De novo gene expression of regulators, which are able to induce joint formation could be a reason for the evolution of an additional joint. Furthermore, a heterotopic shift of regulators responsible for the formation of the primary jaw joint, as well as the alteration of cartilage preserving genes, could explain the partitioning of the lower jaw (Svensson & Haas, 2005). The regulatory gene network responsible for the formation of the primary jaw joint could have become divided into two domains. One of them might have been shifted anteriorly and contributed to the formation of the intramandibular joint. Otherwise it seems possible that downstream targets of regulatory genes involved in primary jaw joint formation acquired a novel function and became involved into the formation of the intramandibular joint.

Regulators involved in primary jaw joint development are known from other vertebrates. In mice *Bapx1* is expressed during embryogenesis within and around the developing malleus and incus. It controls the width of the malleus but is not involved in forming the articulation between these ossicles (Tucker, 2004). In zebrafish the same gene has a regulatory function in forming the articulation between quadrate and articular (Miller *et al.*, 2003). In *X. laevis*, two homologous genes are present, *bapx1* (*nkx3-2*) and *zax* (*nkx3-3*). *Bapx1* or *xenopus bagpipe* is expressed in the mesenchyme surrounding the future jaw joint between the palatoquadrate and Meckel's cartilage (Newman *et al.*, 1997), suggesting a function in the formation of the primary jaw. Previous work has shown, that the absence of *bapx1* led to the loss of the primary jaw joint whereas overexpression of *bapx1* induced ectopic cartilage formation in amphibians (Lukas & Olsson, 2018a, 2018b). However, *bapx1* is not expressed in the area of the intramandibular joint (Newman *et al.*, 1997; Square *et al.*, 2015). *Zax* or *zampogna* expression in *X. laevis* was initially described around the intramandibular joint region (Newman & Krieg, 1999) but recent studies refute these findings (Square *et al.*, 2015), which questions the function of *zax* in intramandibular joint formation. Nevertheless, it may be possible that *zax* expression affects intramandibular joint formation in a cell non-autonomous manner. Additionally, shared functions in joint development with *bapx1* seem possible because of the shared ancestry of both genes.

In order to determine the role of *zax* we describe its temporal expression via qPCR and the effects of functional knockdown of z*ax* on larval cartilage and cranial muscle anatomy and development using two *Zax* antisense oligonucleotides (Zax-MO1 and Zax-MO2). Our findings demonstrate that *zax* is a part of a regulatory gene network, which controls the formation of the intramandibular joint in the lower jaw. It is also involved in the formation of the branchial basket and several cranial muscles, indicating that *zax* is a gene within a regulatory gene network important for the evolution of anuran specific novelties.

Materials and Methods

Xenopus laevis husbandry and manipulation

Xenopus laevis embryos were obtained from our departmental breeding colony. Ovulation was induced by injection of 600 units of human chorionic gonadotropin (HCG) into the dorsal lymph sac of the females. For the induction of amplexus 200 units of HCG were injected into the dorsal lymph sac of the male frogs. Single-pair

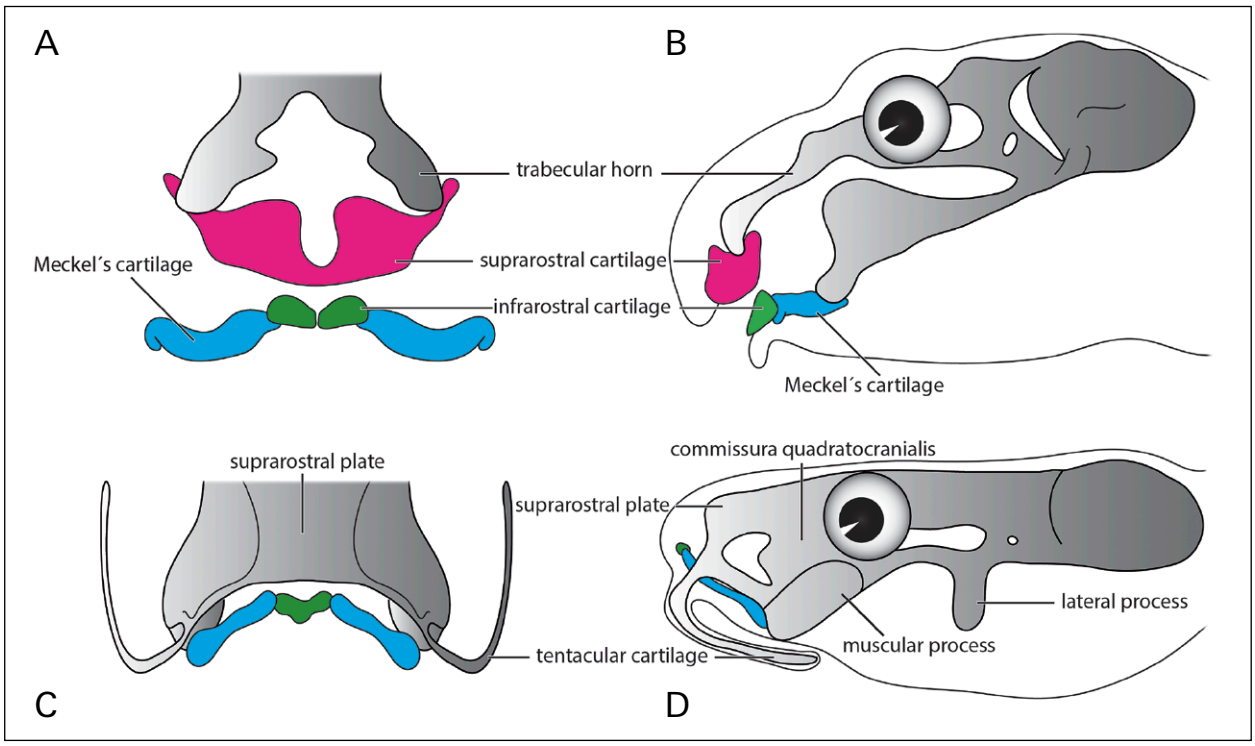

Fig. 1. Overview on the cartilaginous jaw of anuran tadpoles. **A** Generalized jaw parts in frontal (**A**) and lateral (**B**) view with a plate-like suprarostral cartilage, paired infrarostral cartilages and paired, sigmoidal Meckel's cartilage. Composition of the rostrals in the derived *Xenopus laevis* tadpole in frontal (**C**) and lateral (**D**) view. Infrarostrals are fused and Meckel's cartilage is rod-like. The suprarostral cartilage is fused to the trabecular horns and forms the suprarostral plate, which is no longer movable.

mating and egg deposition took place at 15 °C. The eggs obtained were dejellied using 2% cysteinehydrochloride (Merck) and then cultured at 20°C in 0,1× modified Barth's saline (Klein, 2001). Staging was done using the normal table (Nieuwkoop & Faber, 1994).

We knocked down *zax* using the *zax* antisense oligonucleotide (Zax-MO1) 5'-ATGTTAGTGCATAGTATC CAATGGC-3' (ATG complementary sequence underlined) (Gene Tools, USA) with fluorescein at 3' (excitation wavelength 501,5nm) for controlling the proper injection. Fluorescence was checked using an Axiovert S100 (Zeiss, Germany). Injections were performed in 8% Ficoll/0,1× MBS. A total amount of 10 nl with doses of 10–45 ng Zax-MO1 were injected at the one-cell stage. For each dose 30 tadpoles were injected. This was done three times for each dose with changing parental animals. Four hours after injection the embryos were transferred to 0,1× MBS. Once a reproducible phenotype was found we used a second non-overlapping translation blocking Morpholino against *zax* (Zax-MO2) with a different sequence 5'-TATCCAATGGCCGGGAGA AAGGCT-3' to confirm specificity in three further experiments. Eggs were injected with 90–100 ng Zax-MO2 unilateral at the two-cell stage to have an internal control. This high amount was used due to the high G content of the morpholino, which decreases its aqueous solubility and therefore its activity (manufactures advice). A control morpholino oligonucleotide (Co-MO) against human β-globin 5'-CCTCCTACCTCAGTTACAATTTATA-3' (Gene Tools, USA) was injected under the same conditions as a control (10 ng). For studying effects caused by injection and handling, 90 embryos (3 × 30) were only penetrated with the needle at the one-cell-stage without injection. The number of dead and living larvae as well as the number of living and dead larvae with an aberrant phenotype from each experiment was counted each day for up to eight days. Fluorescence of Zax-MO1 injected larvae were checked and only those emitting green light under the fluorescence microscope were used for further investigations.

For the scoring of morphological defects three groups of phenotypes (gut, head, bent axis) were defined (Fig. 4A). If embryos showed ventral oedema, incomplete differentiation of the gut or ventral expansion of the gut, they were considered to be of the gut phenotype. The bent axis phenotype was defined according to the dorsoanterior index of Kao & Elinson (1988). Embryos were considered to show the head phenotype if they had reduced eyes, anterior swelling, reduction or loss of the mouth, or reduction or loss of the entire head. The frequency of all aberrant phenotypes after injection of different doses of morpholino was compared to a uninjected control group and a Co-MO injected group.

Histology

To study the specific effects of *zax* knockdown on cartilage and muscle development we fixed normal larvae and *zax*-MO injected larvae in 4% phosphate-buffered

formalin (PFA) at stages between 35 and 48. These embryos (two normal larvae of each stage and three *zax* phenotypes) were embedded in paraffin, serially sectioned at 7µm thickness using a rotary microtome (HM355 S, Microm) and stained with Azan according to Heidenhain (RIEDELSHEIMER & BÜCHL-ZIMMERMANN, 2015).

CLSM-based 3D-reconstruction

We used whole mount antibody staining according to produce a three-dimensional impression of the changes in cartilage and muscles caused by *zax* knockdown. Antibody staining was carried out according to standard protocol (NAUMANN & OLSSON, 2018). Monoclonal antibodies against newt skeletal muscle (12/101, Monosan) and collagen II (116B3-collagen II, Thermo Fisher Scientific) were used to stain muscles and cartilages, respectively. Alexa 568 (Thermo Fisher Scientific) was used as a fluorescent secondary antibody. Image stacks (10 µm z-plane) were produced using a confocal laser scanning microscope (LSM 510, Zeiss). Based on these stacks, 3D reconstruction of the head was performed using Amira 5.4.0. for surface rendering and Autodesk Maya 2015 for smoothing and rendering of pictures. A total of 37 treated and 14 untreated (one for each stage from 35–48) larvae where examined. Larvae of *Hymenochirus boettgeri* used for 3D-reconstruction were part of our departmental collection.

Quantitative PCR

Quantitative PCR (qPCR) was used to determine the temporal expression of *zax* during *X. laevis* development. RNA was isolated from single whole embryos using QIAzol Lysis Reagent (Qiagen) and purified using RNeasy Mini Kit (Qiagen) according to manufacturer's instructions. RevertAid Transcriptase (Thermo Scientific) was used to synthesize cDNAs from 2 µg of RNA extracted from the embryos. Quantitative PCR was performed using a Stratagene Mx3005P (Agilent Technologies) and one- step qPCR SYBR green kit (Roche). Primers used for amplification of *zax* were 5'-TCTTTGCCCCTATTG CCTCC-3' and 5'-CTTTCTCCGGAGTCAGTGGC-3'. Target gene expression was normalized to the expression level of gene *H4* (*histone 4*) (primer sequence 5'-GACGCTGTCAACCGAG-3' and 5'-CGCCGAAGC-CAGAGTG-3'), which was included in each run. qPCR was performed for the stages 1–45 and the expression of *zax* was calculated relative to stage 10, in which gene expression was considered as basal level. For negative control, a no template (water) control and RT-probe (without RNA template) were used instead of template cDNA. The quantification cycle (C_q) in loq-linear phase of amplification and the RT-PCR efficiency was quantified by using MxPro software version Mx3005P v4.01 Build 369, Schema 80 (Stratagen). Each run was further controlled by analysis of the dsDNA melting curve at the end of each RT-PCR run as well as a control of the resulting amplificates via gel electrophoresis. According to the sample maximization method all three replicates of a sample of the same stage and the same gene were analysed in the same run to minimize run-to-run variations (DERVEAUX *et al.*, 2010).

Results

The temporal expression pattern of *zax*

We used qPCR to determine the temporal expression of *zax*. Transcripts could not be detected until gastrulation (stage 10). *zax* expression started to increase slowly at the mid-neurula stage. From stage 25 to 30 (late tailbud) the expression continued to rise and reached a plateau persisting until the late tailbud stage. With the beginning of chondrification at stage 40, expression increased strongly until stage 45 (Fig. 2).

zax knockdown results in complete loss of head structures

A quantitative analysis of survival and presence of aberrant phenotypes was undertaken. 80% of the control group survived the first 8 days, thus a mortality rate of about 20% was assumed to be normal. Survival of tadpoles did slightly decrease in Co-MO injected (77%) or in needle perforated tadpoles (72%) showing that handling and injecting a volume of 10 nl has a small effect on survival in our morpholino experiments. The more *zax*-MO that was injected, the fewer tadpoles survived and the more phenotypes occurred. Injection of 10 ng Zax-MO1 had no effect on survival or phenotype occurrence whereas injection of 20 ng Zax-MO1 lead to first visible effects. Survival decreased (71%) and different phenotypes occurred. After injection of 45ng Zax-MO1 only 3% of the tadpoles survived for 8 days and 82% displayed different phenotypes. The same trend could be seen after injection of different amounts of Zax-MO2 (Fig. 3A).

No phenotypes were observed in the untreated control group. The bent axis phenotype only occurs infrequently and is not considered to be a specific effect of *zax* knockdown. It can be observed from NF25 onwards. One gut phenotype observed was a translucent oedema ventral to the anterior gut, which in most cases disappeared during further development (Fig. 4B, bottom). This phenotype is considered to be an effect caused by perforation during injection because it is evenly distributed among all injections (except after injection of 10 ng Zax-MO1) but did not appear in untreated larvae. The occurrence of the head phenotype increased with the amount of Zax-MO1 injected and can be observed from NF40 onwards. It starts at 20 ng with a swollen mouth region. 4% of the treated tadpoles show this kind of deformation. The higher the amount, the more crucial the effect and the more tadpoles are affected. After injection of 30 ng 13% display a head phenotype where the mouth opens incom-

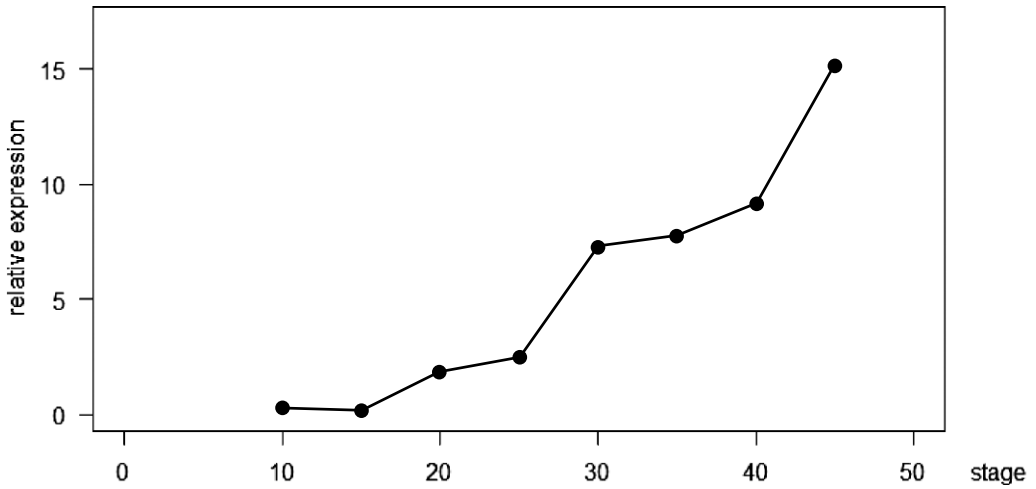

Fig. 2. Relative expression of *zax* normalized to the expression level of the *H4* (*histone 4*) gene. Transcripts could not be detected before stage 10. Expression increased at stage 25 before chondrogenesis has started. The increase at stage 40 marks the beginning of the differentiation of the cartilage condensation, implying a role for *zax* both in the initiation of chondrogenesis and in the differentiation of chondrocytes.

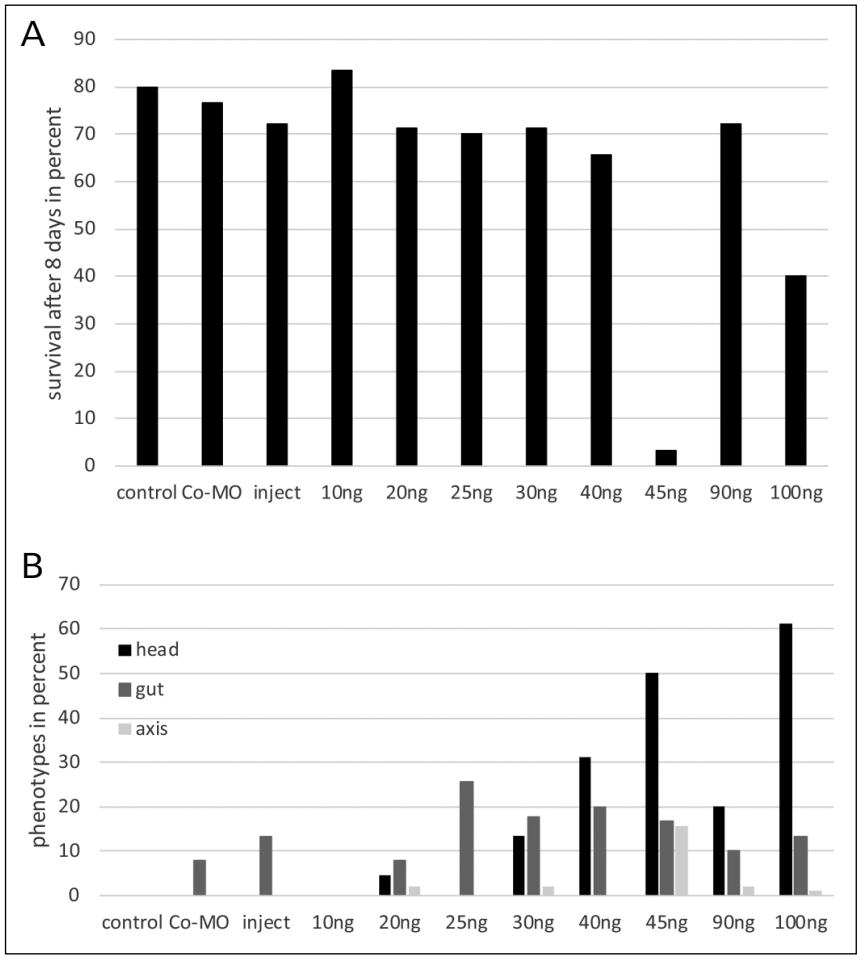

Fig. 3. A) Quantitative analysis of survival after injection of Zax-MO1 at the one cell stage and of Zax-MO2 unilaterally in two-cell stage *Xenopus laevis* until eight days. **B**) Distribution of different phenotypes after injection of different doses of Zax-MO. 10–45 ng are the doses of Zax-MO1 injected, 90 ng and 100 ng those of Zax-MO2, control describes the normal development without injection, Co-MO the injection of 10 ng control morpholino and injected the sham operation (perforation with a needle without injection). Phenotypes were identified as described in Materials and Methods (see *Xenopus* husbandry and manipulation for details).

pletely. Eyes, mouth or the entire head failed to develop after injection of 45ng (Fig. 4C). Injections of 40 ng Zax-MO1 showed the best payoff between head deformation (31%) and survival (65%). 20% of tadpoles developed a head phenotype after injection of 90 ng Zax-MO2 and 61% after injection of 100 ng (Fig. 3B).

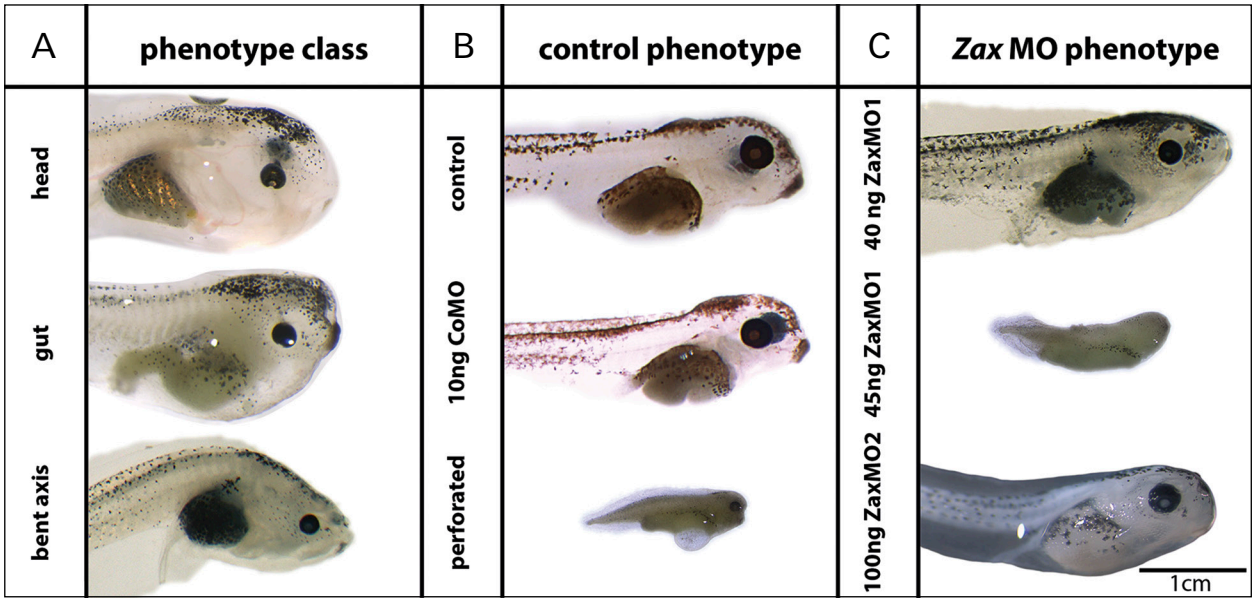

Fig. 4. Phenotypes displayed at different stages after injection of different doses of Zax-MO. **A**) Phenotype classes as described in Materials and Methods (NF44 each). **B**) Control phenotypes with uninjected tadpole on top (NF44), CoMo injected in the middle (NF44) and needle perforated at the bottom (NF37). No difference can be seen between uninjected and CoMO injected larvae, both develop normally. Larvae treated with the needle sometimes display a ventral oedema, which disappears during further development. This oedema also occurs in *zax*-MO and Co-MO injected specimens. **C**) Phenotypes displayed after *zax* knockdown. Larvae injected with 40 ng Zax-MO1 (top) show a protruding, swollen mouth region and are unable to open the mouth (NF45). 45ng Zax-MO1 injected embryos (middle) show different types of loss of head structures (NF ~ 36). 100 ng Zax-MO2 injected larvae resemble the tadpoles treated with 40 ng Zax-MO1 (NF42).

In our further investigations of the effects of *zax* knockdown we performed injections of 40 ng Zax-MO1 and 100 ng Zax-MO2, which both reliably produced specific, reproducible and numerous head phenotypes. The development of these phenotypes showed a delay of about two stages compared to the normally developing untreated control group.

zax knockdown results in defects of cartilage formation

The following description of cartilage defects is based on tadpoles treated with 40 ng Zax-MO1 or 100 ng Zax-MO2, respectively. 31% of 40 ng Zax-MO1 and 61% of 100 ng Zax-MO2 injected tadpoles developed the head phenotype with a swollen mouth region and an incomplete mouthopening (Fig. 3B). The neural crest-derived infrarostral, Meckel's cartilage, ceratohyal and the branchial basket are all malformed after *zax*-knockdown. Dorsal neural crest-derived as well as mesoderm derived cartilages are not malformed. Chondrocranium development is delayed. Normally developed larvae fixed at the same time as the Zax-MO1 treated larvae display all features of a stage 48 tadpole, including a well-developed tentacular cartilage, a closed basicranial fenestra and otic capsules fused to the wall of the braincase (Fig. 5A, B). The Zax-MO1 treated larva instead shows traits typical of stage 45–46 larvae (Fig. 5D, E). A tentacular cartilage extending between the suprarostral plate and the processus cornu quadratis lateralis of the palatoquadrate is not present. The rostral part of the suprarostral plate is characterized by a broad u-shaped notch and the cornuae trabeculae are less developed. A subocular fenestra is present, but extends further caudally compared to control specimen. The basicranial fenestra is not closed and the otic capsules are only slightly fused to the wall of the braincase. Also, the connection of the otic capsules to the processus lateralis of the palatoquadrate is not present. The otic capsules themselves display no malformation. Because of the delayed development they look similar compared to the otic capsules of control larvae at stage

Fig. 5. Three-dimensional reconstruction of the chondrocranium and the cranial muscles of Zax-MO1 and Zax-MO2 injected larvae. Both injections lead to delayed development. **A**) Chondrocranial morphology of 40 ng Zax-MO1 injected tadpole (right) and control specimen (left) in dorsal view. **B**) 40 ng Zax-MO1 injected tadpole (right) and control specimen (left) in ventral view. Injected larvae display conditions found at stage 46 whereas uninjected larvae are at stage 48 (both are fertilized and fixed at the same time). Injected larvae are shorter and laterally compressed compared to controls. Several differences, such as the fusion of Meckel's cartilage and the infrarostral cartilage as well as the malformation of the branchial basket can be identified. Ceratobranchial IV is covered by ceratobranchial II from this point of view. **C**) Cranial muscles in injected (right) and uninjected (left) *Xenopus laevis* larvae in ventral view at stage 48. The phenotype displays various malformations of muscles such as fusion (gh+sr, gh+im), shifted insertion (gh) frayed appearance (ab, ih, im) and disordered pathways (so, im). **D**) Morphology of the 40 ng Zax-MO1 injected tadpole (right) in comparison to a stage 46 NF normal developed tadpole (left) in dorsal view. **E**) 40 ng Zax-MO1 injected tadpole (right) and stage 46 NF tadpole (left) in ventral view. The injected larvae display most of the traits of a stage 46 tadpole including the shape of the ceratohyal, the

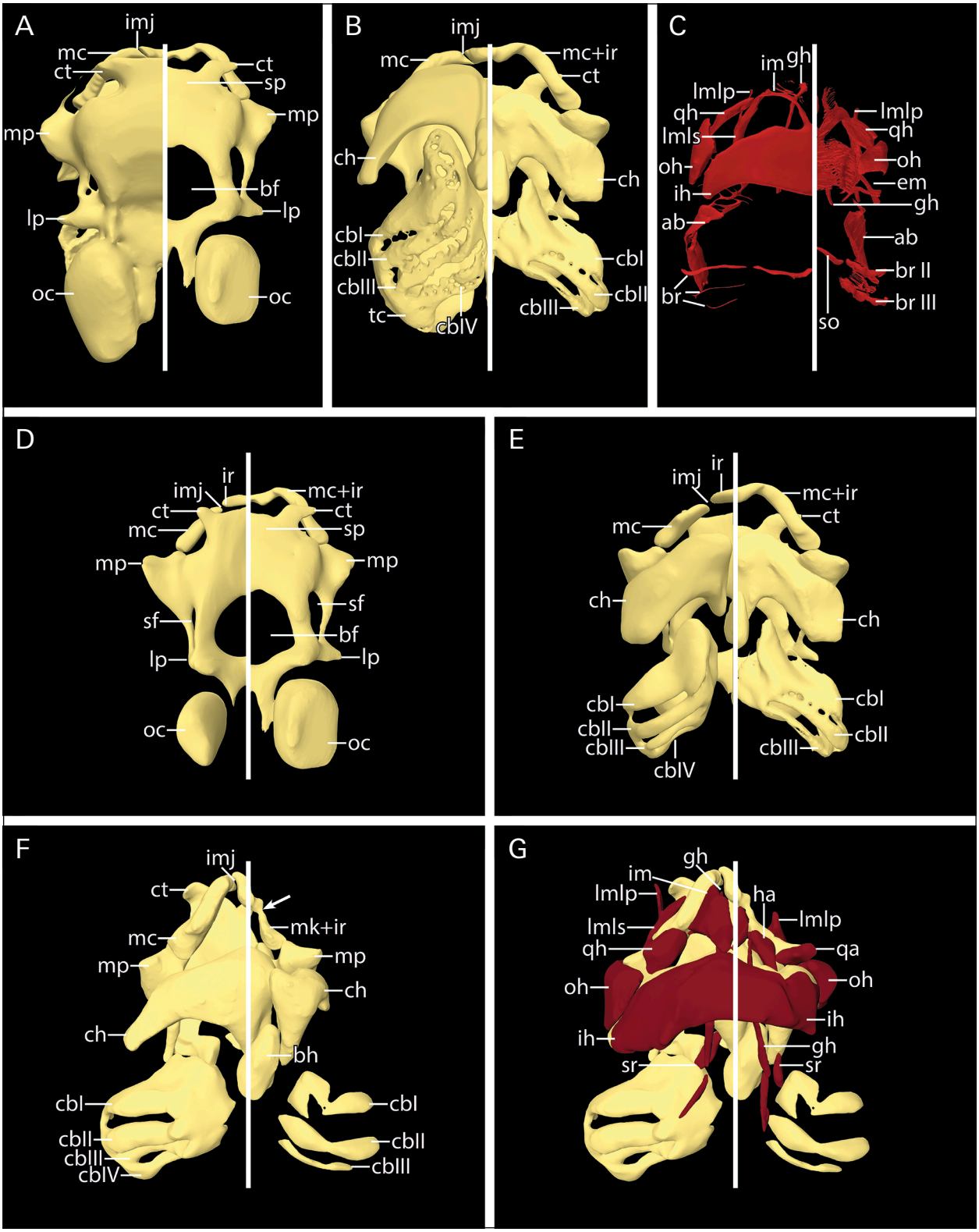

open basicranial fenestra and the missing tentacular cartilage. **F**) Chondrocranium of a 100 ng Zax-MO2 unilateral injected tadpole at stage 46 with the injected side on the right and the uninjected one on the left. Fusion of infrarostral and Meckel's cartilage is also visible (arrow). Additionally, the ceratohyal is malformed and the ceratobranchial IV is missing. **G**) Cranial muscles of a 100 ng Zax-MO2 unilaterally injected tadpole at stage 46 with the injected side on the right and the uninjected side on the left. Remarkable is the loss of the insertion of the m. geniohyoideus on the infrarostral and the separation of m. quadratoangularis and m. hyoangularis. Abbreviations: ab, mm. levator arcuum branchialium I–IV; bf, basicranial fenestra; bh, basihyal; br, mm. constrictors branchialis II–IV; cbI–IV, ceratobranchial I–IV; ch, ceratohyal; ct, cornua trabecula; em, eyemuscles; gh, m. geniohyoideus; ha, m. hyoangularis; ih, m. interhyoideus; im, intermandibularis; ir, infrarostral cartilage; mc, Meckel's cartilage; lmlp, m. levator mandibulae longus profundus; lmls, m. levator mandibulae longus superficialis; lp, lateral process; mp, muscular process; oc, otic capsule; oh, m. orbitohyoideus; qa, m. quadratoangularis; qh, m. quadrato-hyoangularis; sf, fenestra subocularis; so, m. subarcualis obliquus; sr, m. subarcualis rectus I; tc, tentacular cartilage; tc, terminal commissure.

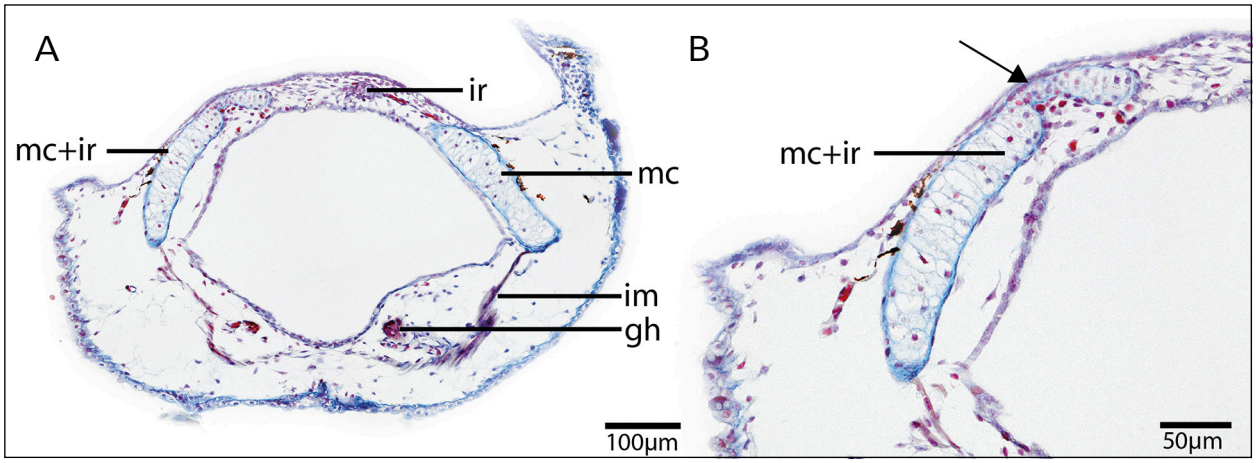

Fig. 6. Histological cross-sections through the head of a Zax-MO1 injected *Xenopus laevis* larva. **A**) Frontal section through the anterior part of the head. Because of a slightly skewed sectioning the fused cartilage can only be seen on one side. Notice the great distance between infrarostral cartilage and m. geniohyoideus. **B**) The connection between Meckel's cartilage and the infrarostral in detail (arrowheads). No intramandibular joint is visible. Abbreviations: gh, m. geniohyoideus; im, m. intermandibularis; ir, infrarostral cartilage; mc, Meckel's cartilage.

46 (Fig. 5D). In Zax-MO1 treated larvae the chondrocranium shows a slight left-right asymmetry (Fig. 5A, B). A developmental delay of two stages can also be seen in the Zax-MO2 unilaterally injected larvae. The uninjected control side is much larger than the injected side with well-developed chondrocranial structures (Fig. 5F). It shows the same malformations as those on both sides in bilaterally injected tadpoles. The uninjected side shows the same normal morphology as seen in control specimens. It resembles a stage 45 tadpole, whereas the injected side show traits of stage 43. This leads to an asymmetric morphology, where the suprarostral plate proceeds diagonally and the ceratohyal on the control side extends over the midline of the larva.

The larval anuran lower jaw normally consists of two mandibular neural crest stream-derived elements, the infrarostral and Meckel's cartilage. In the control specimen, Meckel's cartilage is sigmoid shaped and articulates through the intramandibular joint with the fused infrarostral cartilages. After Zax-MO1 knockdown, Meckel's cartilage is a continuous cartilage, which lacks an intramandibular joint (Figs. 5, 6B). The normal shape of Meckel's cartilage is lost after knockdown. Instead the lower jaw consists of one continuous slightly W-shaped cartilage without any visible intramandibular joint. A caudal projection is seen at the midline (Figs. 6, B, and D). Meckel's cartilage is straighter and caudally shortened compared to controls. It also extends laterally over the margin of the cornuae trabeculae on the right side. On the left side Meckel's cartilage extends dorsally and is shortened. The retroarticular processus is not well developed, but the articulation with the palatoquadrate is present (Fig. 7D). Zax-MO2 knockdown also lead to the absence of the intramandibular joint (Fig. 7C, E). An intramandibular joint is present on the control side and Meckel's cartilage develops normally.

The hyoid neural crest stream-derived ceratohyal cartilage displays a mild deformation. The lateral processus is broader and has a horizontal orientation instead of a more vertical one. On its anterior margin, the ceratohyal usually has a consistent rounding, whereas the Zax-MO injected cartilage is uneven. The right part of this paired cartilage is reduced in size. The fusion is incomplete and the left part extends over the midline of the larva (Fig. 7B). After Zax-MO2 injection the ceratohyal is severely deformed (Fig. 5F, 7C). It is dramatically reduced in size and shows a rectangular bend between the anterolateral process and the lateral process.

The branchial basket is severely malformed after Zax-MO1 treatment. The terminal commissure is bent laterally and extends dorsally in the direction of the otic capsules. The slit between ceratobranchial I and II is nearly closed on the left side and fails to develop on the right side. The ceratobranchial IV is translocated anteriorly and dorsally and placed dorsal to ceratobranchial II. After Zax-MO2 injection no terminal commissure is present and the ceratobranchial IV is missing. The basihyal and the otic capsules are normally developed in both cases (Figs. 4 and 6).

zax knockdown affects cranial muscle development

Several cranial muscles with different embryonic origins display malformations. Insertions are changed, differentiation is incomplete and some muscles are frayed. The extrinsic eye muscles develop normally. Because of the laterally compressed shape of the head phenotype, the musculature is less broad than in the control tadpole. The development of the musculature is delayed by three stages (Fig. 5C, E).

Mandibular arch musculature

The m. levator mandibulae group differentiates very late in development (ZIERMANN & OLSSON, 2007) and some

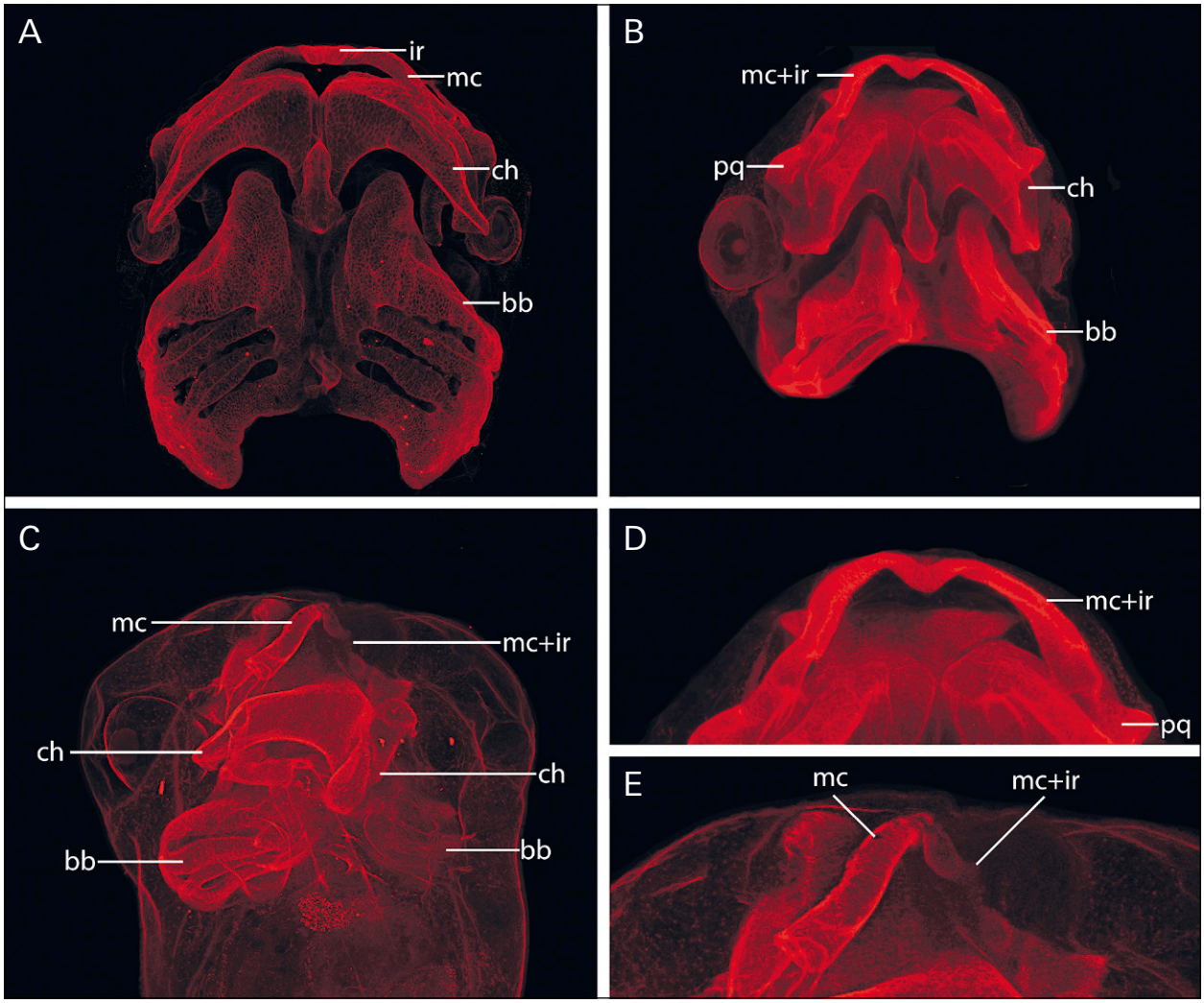

Fig. 7. Maximum intensity projections of whole-mount immunolabeled *Xenopus laevis* larvae in ventral view. **A**) shows a control larva at stage 48. **B**) shows a Zax-MO1 injected (40 ng) larva with a slight left-right asymmetry. The branchial basket is severely deformed. Meckel's cartilage and infrarostrals are fused and form a nearly U-shaped lower jaw. **C**) Zax-MO2 unilateral injected (100 ng) larva with the injected side on the right and the uninjected side on the left. Infrarostral and Meckel's cartilage are fused on the injected side, whereas on the control side the intramandibular joint is present. **D**) Detailed view of the lower jaw of the larva in B. **E**) Detailed view of the lower jaw of the larva in C. Abbreviations: bb, branchial basket; ch, ceratohyal; ir, infrarostral cartilage; mc, Meckel's cartilage; pq, palatoquadrate.

muscles of this group could not be observed, neither in treated nor in control tadpoles. The m. lev. mand. longus superficialis et profundus both originate from the suborbital bar. Posteriorly, the different portions of these muscles could not be distinguished. Cranially, the profundus portion extends laterally and inserts at the distal tip of the suprarostral plate, next to the tentacular cartilage. Although the phenotype lacks this cartilage, the profundus portion develops well, but extends in the wrong direction in treated specimen (Fig. 5C). The superficialis portion is stout and proceeds straight rostrally to insert on the lateral surface of Meckel's cartilage. In the treated tadpoles this muscle is thickened, bends proximally and attaches further dorsally than in control tadpoles. The m. intermandibularis originates ventrally on each side at Meckel's cartilage, and the parts from each side meet in the median raphe. The entire muscle consists of a single layer of fibres (Candioti, 2007) and is slightly v-shaped. In the head phenotype caused by Zax-MO1 injection this muscle is disordered. Single fibres fail to insert at Meckel's cartilage and are frayed. The muscle extends anteriorly and displays a more distinct v-shape than in control tadpoles (Fig. 5C). After Zax-MO2 treatment the muscle is much smaller on the injected side than on the control side but it attaches normally on the part of the fused lower jaw element, which appears to be the Meckel's cartilage portion (Fig 4G).

Hyoid arch musculature

The m. quadrato-hyoangularis is a fused muscle extending from the ventral surface of the palatoquadrate and the dorsal surface of the ceratohyal to the lateral edge of Meckel's cartilage. The origin at the ceratohyal is lost and the insertion is shifted dorsally in Zax-MO1 treated tadpoles (Fig. 5C). Zax-MO2 treated tadpoles surprisingly develop two distinct muscles, the m. quadratoan-

gularis, which extends between the palatoquadrate and Meckel's cartilage and the m. hyoangularis connecting the ceratohyal and Meckel's cartilage (Fig. 5G). In uninjected as well as in Zax-MO1 treated tadpoles these two muscles share their insertion but the m. hyoangularis inserts at the anterior margin whereas the m. quadratoangularis inserts at the lateral edge of Meckel's cartilage. The m. orbitohyoideus connects the muscular process and the lateral process of the ceratohyal. Normally it proceeds diagonally because the muscular process is placed anterior to the ceratohyal. Zax-MO1 head phenotypes have a vertically oriented m. orbitohyoideus, that is smaller than normal. The m. interhyoideus is a broad, flattened muscle, which extends between both lateral processi of the ceratohyal. It is thickened and u-shaped after injection of Zax-MO1, probably as a result of the changes in the shape of the ceratohyal.

Branchial arch musculature

All muscles in this group are affected by the knockdown of *zax* owing to the malformation of the branchial basket. m. subarcualis obliquus (also known as m. transversus ventralis II) normally extends laterally from the median aponeurosis to the ceratobranchialia II. After Zax-MO1 knockdown its pathway is curved and its insertion is shifted laterally. The m. constrictor branchialis II and III originate normally but their insertion is shifted dorsally. The m. constrictor branchialis IV is located behind m. constrictor branchialis III due to the malformation of the associated ceratobranchial IV. The fused m. levatores arcuum branchialium I–IV develop normally but some fibres are frayed. The subarcualis rectus I normally extends between the medial margin of the ceratohyal and the proximal part of ceratobranchial I. In Zax-MO1 depleted tadpoles the muscle is fused at its origin to the m. geniohyoideus and the insertion on the ceratohyal is lost, whereas in Zax-MO2 treated embryos it develops normally (Fig. 5C, E).

Hyobranchial musculature

M. geniohyoideus is a paired muscle that originates at the hypobranchial plate near the ceratobranchial II and inserts on the infrarostral. It is a thin, elongated muscle that only consists of a few fibres. After Zax-MO1 knockdown this muscle displays a peculiar phenotype. On its way anteriorly from its origin at least one strand penetrates both the m. interhyoideus and the m. intermandibularis. The insertion at the infrarostral cartilage is lost and the strands end abruptly in condensed tissue (Fig. 5C). Zax-MO2 induced head phenotype shows a similar condition. The strand of the m. geniohyoideus from the injected side fails to attach to the cartilage but does not penetrate another muscle. The strand from the control side inserts laterally near the gap, which forms the intramandibular joint on the fused infrarostral and Meckel's cartilage (Fig. 5G). Both strands originate from the median part of ceratobranchial II.

Discussion

Neural crest-derived cartilage development depends on *zax* expression

In comparison to normal cartilaginous development described before (LUKAS & OLSSON, 2018c) the functional knockdown of *zax* causes a wide range of malformations in the developing cranial skeleton. When comparing the temporal expression pattern and the phenotypes produced by knockdown, several functions of *zax* during development seem possible. The first increase of *zax* expression takes place at stage 20 NF. At this time neural crest cells start to migrate (SADAGHIANI & THIÉBAUD, 1987). (1) Due to the fatal head phenotype displayed at doses of 45ng Zax-MO1 *zax* could play a role in early development because small changes at the beginning of development can lead to large changes in later developmental stages. (2) N*kx 3.2* (a homologue of *Xbap*) is required at the onset of chondrogenesis for the proliferation of chondrocytes (GOLDRING *et al*., 2006). It is activated when chondroblasts appear and is less expressed after proliferation of chondrocytes. Temporal and spatial expression of *zax* correlates with chondrocyte differentiation in *X. laevis* but expression is not decreased after proliferation as shown for *nkx 3.2* (*bapx1*) (GOLDRING *et al*., 2006). *Zax* may have a regulating function in chondrocyte proliferation, as does *bapx1* (YAMASHITA *et al*., 2009). (3) Additionally, it may have acquired a function during early neural crest cell migration or further cartilage development. A knockdown of *zax* may has lowered the number of cells in the neural crest derived anlagen, which then led to malformations or slowed development. (4) The mesodermal origin of the basibranchial and the otic capsules is a common feature of anurans (SADAGHIANI & THIÉBAUD, 1987; OLSSON & HANKEN, 1996). Interestingly, these structures are not affected by the functional knockdown of *zax*. This leads to the assumption that neural-crest derived cells require *zax*-dependent signals for proper development whereas mesoderm-derived cells do not. Although the differences between normally developed and *zax*-depleted chondrocrania seem obvious, these are not considered to be malformed because the differences are caused by the delayed development of the morpholino-injected larvae. All major processes are present and the primary jaw joint develops normally. All malformations can be found on the ventral side of the head in structures derived from the neural crest streams. The mandibular neural crest stream-derived cartilages are fused. Hyoid stream-derived ceratohyal shows, depending on the morpholino injected, mild to severe changes in shape and size and the branchial stream-derived branchial basket is seriously malformed, including fusion of ceratobranchials (Zax-MO1) or loss of ceratobranchials (Zax-MO2). It is obvious that only ventral neural crest-derived cartilages are malformed. Therefore, a dorsoventrally operating regulatory gene network can be assumed to regulate this morphogenesis. (5) Dorsally,

zax seems to have no regulating function, which would correlate with the expression pattern, or redundant pathways are active controlling the correct development of the dorsal parts.

Cranial muscle morphogenesis requires *zax*

Changes in the shape and insertion of muscles after *zax* knockdown correlate well with the malformations of the cartilaginous head skeleton in *X. laevis* larvae and only ventral muscles are malformed. This is caused by the correlated development of muscles and cartilage. Neural crest cells that contribute to the cartilage define the shape and size of developing muscles (Rinon *et al*., 2007; Tokita & Schneider, 2009). Shortened muscles such as the m. geniohyoideus could appear because of indirect effects of the perturbed development of neural crest-derived cells, which are obviously affected by *zax* knockdown. Neural crest extirpation experiments in the Mexican axolotl (*Ambystoma mexicanum* Shaw, 1798) show that muscles differentiate normally in the absence of neural crest cells, but fail to extend towards their normal insertions. Furthermore, a frayed appearance was observed (Ericsson *et al*., 2004). These results correlate well with our observations in *zax*-depleted larvae. The delay of the m. intermandibularis and m. interhyoideus follows the malformations of Meckel's cartilage and the ceratohyal, respectively. The spatial and temporal pattern of normal muscle development has been described (Ziermann & Olsson, 2007). In comparison, the musculature in Zax-MO depleted tadpoles shows a developmental delay of about three stages as does the entire larva. Zax-MO2 treatment leads to the separation of the m. quadratohyoangularis into the m. quadratoangularis and the m. hyoangularis, with a shifted insertion on Meckel's cartilage of the m. hyoangularis. This could be a result of the massive deformation of the ceratohyal or its shifted position. Interestingly, in Zax-MO1 treated larvae the origin of the m. quadratohyoangularis on the ceratohyal is lost. In light of the results of Zax-MO2 experiments, it seems that the m. hyoangularis is lost and only the m. quadratoangularis exists in Zax-MO1 tadpoles. The shortening of the m. geniohyoideus, the loss of its insertion at the infrarostral cartilage and its fusion at the origination to the m. subarcualis rectus is an interesting malformation in Zax-MO1 treated tadpoles. There is a correlation between the development of several cranial muscles and the chondrogenesis of skeletal elements (McClearn & Noden, 1988). Cells from connective tissues migrate into muscle anlagen and separate them. This does not happen in the area of the future origination of m. geniohyoideus and m. subarcualis rectus in Zax-MO1-treated tadpoles. The normal development of the ceratobranchial cartilage leads to a separation of both anlagen (Ziermann & Olsson, 2007). After knockdown of *zax* the ceratobranchial cartilage is malformed and the entire branchial basket is smaller than normal. The close relationship of the two anlagen and the Zax-MO1 affected connective tissue, which does not form correctly, leads to a failure of separation. Such malformations could also be seen in FoxN3-MO-injected *X. laevis* larvae (Schmidt *et al*., 2011). It has been shown that FoxN3 knockdown also leads to downregulation of *zax* (Schuff *et al*., 2007). Therefore, it is not surprising that functional knockdown of *zax* leads to similar malformations. A regulatory gene network could be present where *zax* is a downstream target of FoxN3 and they are both parts of a neural-crest cell regulating network.

zax and its potential role in the origin of evolutionary novelties

From an evo-devo perspective, it is an important observation that only neural crest-derived structures are affected by the knockdown of *zax*. Interestingly, anuran-specific innovations, e.g. the infrarostral cartilage and the filigreed gill basket, show the most drastic malformations in *zax*-depleted tadpoles (Figs. 4 and 6). These malformations resemble the conditions of homologous structures in salamanders and are more severe than malformations after the knockdown of the paralogous gene *bapx1* (Lukas & Olsson, 2018a). Salamanders have no rostrals but an elongated, U-shaped Meckel's cartilage similar to the one displayed by *zax*-Morphants. The gill basket is a simple arrangement of two hypobranchials and four ceratobranchials, which forms a V-shaped basket connected by two basibranchials in the midline. The slight V-shaped basket of Zax-MO depleted tadpoles together with a general simplification of this structure is similar to the salamander condition. *Hymenochirus boettgeri*, a small frog closely related to *X. laevis* also has a reduced branchial basket, which only consists of two ceratobranchials (Fig. 8). Additionally, the tadpole of this frog has a continuous, U-shaped lower jaw without an infrarostral cartilage (Rose, 2014). Based on our morphological results it seems possible that alterations in *zax* expression could have led to the absence of the intramandibular joint and a stepwise reduction of ceratobranchials within the stem line of *H. boettgeri*. This hypothesis needs to be tested by investigating *zax* expression patterns or *zax* upregulation experiments in *H. boettgeri*. FoxN3-depleted tadpoles also display a malformed intramandibular articulation and a gill basket that resembles homologous structures in salamanders (Schmidt *et al*., 2011). Furthermore, it has been shown that FoxN3 directly influences the expression of Nkx genes such as *zax* (Schuff *et al*., 2007). Thus, the similarity of malformations is not surprising but implies that *zax*, even if regulated by FoxN3, plays a role in the gene regulatory network controlling the development of anuran-specific novelties.

The evolution of the vertebrate jaw includes the evolution of a jaw joint. This starts with an unjointed condition in the agnathan ancestor. In the first branchial arch of lampreys, no gnathostome-like expression of *Bapx1* is present (Cerny *et al*., 2010), but in zebrafish and chicken it is involved in primary jaw joint development (Miller *et al*., 2003; Wilson & Tucker, 2004). A homologous gene *zax*, which evolved through genome duplication (Newman & Krieg, 1999), has been suggested as a candidate

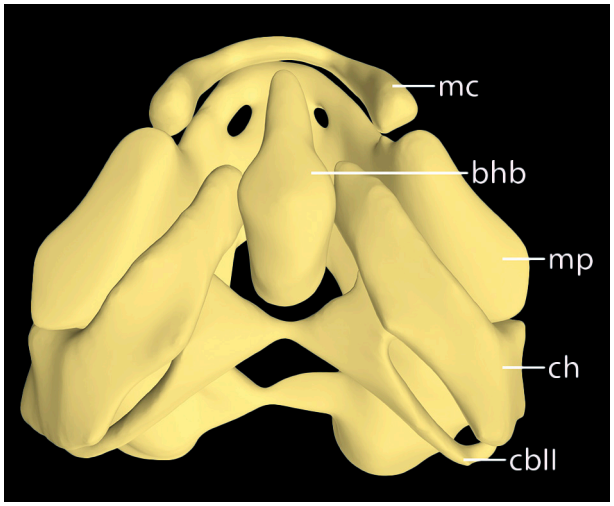

Fig. 8. Three-dimensional reconstruction of the larval head of *Hymenochirus boettgeri*. Noticeable are the continuous lower jaw without intramandibular joints and the branchial basket only consisting of ceratobranchial I and II (cbI is situated under the ceratohyal and cannot be seen). Abbreviations: bhb, basihyobranchiale; cbII, ceratobranchiale II; ch, ceratohyale; mc, Meckel's cartilage; mp, muscular process.

gene for the development of the intramandibular joint (Svensson & Haas, 2005) because it is expressed in the area of the future infrarostral cartilage. *Zax* is expressed in the ectoderm around the stomodeum at stage 37 (Square *et al.*, 2015). This *zax* expressing ectodermal region arises at stage 32 and overlies the future infrarostral and intramandibular joint mesenchyme before it splits into two stripes over each first branchial arch. Expression ends around stage 41 just about when *GDF5* expression is detectable in and around the intramandibular joint (Square, pers. comm.). According to our experiments, it is possible that *zax* either directly turns on *GDF5* or somehow initiates a cascade that turns on *GDF5*, which then specifies the intramandibular joint. Thus, *zax* seems to be acting in a cell non-autonomous way because it is not expressed in the joint tissue itself, but instead overlying it before it develops. This model is consistent with our experiments, which strongly indicate that specification of the intramandibular joint occurs in a *zax*-dependent manner.

The temporal expression pattern in *X. laevis* is consistent with the development of the joint. Expression starts to increase when the first chondrocytes appear and continues when cartilages and joint develop in the head of *X. laevis* embryos. Joint formation has been investigated in limb development, where it starts with the formation of an interzone, the future place of the joint. How this zone is induced remains unknown. In a second phase, specification of this region is mediated through *wnt14* and *GDF5* (Khan *et al.*, 2007). This leads to the separation of the cartilage and the emergence of two distinct structures and the joint cavity. Morphogenesis forms the distal end of the one and the proximal end of the other part, with the result that both ends together form a joint (Pitsillides & Ashhurst, 2008; Dy *et al.*, 2010). *Bapx1* positively regulates the expression of *GDF5*, which defines the future position of the primary jaw joint (Miller *et al.*, 2003). *GDF5* is also expressed in the region of the future intramandibular joint and is independent of *bapx1* expression there (Square *et al.*, 2015), implying that it is involved in joint development. The loss of the intramandibular joint after functional knockdown of *zax* and the expression pattern indicates a role for *zax* in the development and evolution of this joint. We suggest that *zax* defines the position of the intramandibular joint by regulation of *GDF5* or one of its upstream regulators, mimicking the ancestral role of *bapx1* which regulates *GDF5* to develop the primary jaw joint. This function could be conserved through the duplication event at the origin of anurans and an expression shift could lead to the formation of a new joint.

Another possibility is that the intramandibular joint is homologous to joints found on more posterior arches at the level of hypohyal-ceratohyal and hyobranchial-ceratobranchial in fish and salamanders. If this is the case, this joint (including its regulatory gene network) could be a primitive feature of all vertebrate pharyngeal arches. The joint itself could have been lost or the gene expression making it was turned off when the first arch skeleton evolved into jaws. Switching the expression back on again in the frog ancestor could have led to evolution of the infrarostral in anuran tadpoles (Rose, pers. comm.).

The loss of the insertion of the m. geniohyoideus on Meckel's cartilage may have caused the loss of the intramandibular joint. As recently shown in zebrafish, muscle activity is required for joint morphogenesis (Brunt *et al.*, 2015). Normally the m. geniohyoideus is present when the infrarostral cartilage begins to form. It is possible that the loss of muscle attachment and thus the loss of mechanical impact on the infrarostral cartilage caused the loss of the intramandibular joint.

What are the genetic changes that lead to morphological variation and thus to evolutionary novelties? In our present investigation we removed *zax* from its gene regulatory network through functional knockdown. The received phenotype shed light on a potential role for *zax*. We have shown that alteration of an existing network can lead to morphological variation that can result in evolutionary novelties. If this variation becomes adaptive and heritable it is one way to generate evolutionary novelties. Just like the lamprey mandibular arch pattern was altered and *bapx1* invaded to form the primary jaw joint, the network to which *zax* belongs could have invaded the anuran first arch to form the intramandibular joint.

Acknowledgements

We are very grateful to Katja Felbel for technical support. This project was funded by the Deutsche Forschungsgemeinschaft (Grant Number: DFG-OL 134/10-2 to LO). JS was supported by the Konrad-Adenauer-Stiftung and PL by the Studienstiftung des deutschen Volkes. The authors declare no conflict of interest. We wish to thank Christopher S. Rose, Tyler Square, Mats E. Svensson, Benjamin Naumann, and an anonymous reviewer for very thoughtful comments that helped us improve the paper.

Author contributions

PL, JS, and LO developed the concept and design of the study. PL was responsible for the experimental procedures including acquisition of the qPCR and RT-PCR data, *zax*-MO injections, scoring of the surviving embryos and phenotypes, immunostainings and 3D reconstructions as well as histology. Analysis and interpretation of the data mentioned was mainly done by PL, who was also responsible for the drafting of the manuscript and its final form. JS was involved in analysing and interpreting the data and JS and LO critically revised the manuscript.

References

Beverdam, A. Merlo, G. R., Paleari, L., Mantero, S., Genova, F., Barbieri, O., Janvier, P. & Levi G. (2002). Jaw transformation with gain of symmetry after Dlx5/Dlx6 inactivation: Mirror of the past? *Genesis*, **34**, 221–227.

Brunt, L. H., Norton, J. L., Bright, J. A., Rayfield, E. J. & Hammond, C.L. (2015). Finite element modelling predicts changes in joint shape and cell behaviour due to loss of muscle strain in jaw development. *Journal of Biomechanics*, **48**, 3112–3122.

Candioti, m. F. V. (2007). Anatomy of anuran tadpoles from lentic water bodies: systematic relevance and correlation with feeding habits. *Zootaxa*, **1600**, 1–175.

Cerny, R., Cattell, M., Sauka-Spengler, T., Bronner-Fraser, M., Yu, F. & Medeiros, D. M. (2010). Evidence for the prepattern/cooption model of vertebrate jaw evolution. *Proceedings of the National Academys of Sciences of the USA*, **107**, 17262–17267.

Depew, m. J. (2002). Specification of jaw subdivisions by Dlx genes. *Science*, **298**, 381–385.

Derveaux, S., Vandesompele, J. & Hellemans, J. (2010). How to do successful gene expression analysis using real-time PCR. *Methods*, **50**, 227–230.

Dy, P., Smits, P., Silvester, A., Penzo-Méndez, A., Dumitriu, B., Han, Y., de la Motte, C. A., Kingsley, D.M. & Lefebvre, V. (2010). Synovial joint morphogenesis requires the chondrogenic action of Sox5 and Sox6 in growth plate and articular cartilage. *Developmental Biology*, **341**, 346–359.

Ericsson, R., Cerny, R., Falck, P. & Olsson, L. (2004). Role of cranial neural crest cells in visceral arch muscle positioning and morphogenesis in the Mexican axolotl, *Ambystoma mexicanum*. *Developmental Dynamics*, **231**, 237–247.

Goldring, m. B., Tsuchimochi, K. & Ijiri, K. (2006). The control of chondrogenesis. *Journal of Cellular Biochemistry*, **97**, 33–44.

Gross, J. B. & Hanken, J. (2008). Segmentation of the vertebrate skull: neural-crest derivation of adult cartilages in the clawed frog, *Xenopus laevis*. *Integrative and Comparative Biology*, **48**, 681–696.

Khan, I. M., Redman, S. N., Dowthwaite, G. P., Oldfield, S. F. & Archer, C. W. (2007). The development of synovial joints. *Current Topics in Developmental Biology*, **79**, 1–36.

Klein, P. (2001). Early development of *Xenopus laevis*: a laboratory manual. *The Quarterly Review of Biology*, **76**, 1–236.

Lukas, P. & Olsson, L. (2018a). *Bapx1* is required for jaw joint development in amphibians. *Evolution & Development*, **20**, 192–206.

Lukas, P. & Olsson, L. (2018b). Bapx1 upregulation is associated with ectopic mandibular cartilage development in amphibians. *Zoological Letters*, **4**, 16.

Lukas, P. & Olsson, L. (2018c). Sequence and timing of early cranial skeletal development in *Xenopus laevis*. *Journal of Morphology*, **279**, 62–74.

McDiarmid, R. W. & Altig, R. (1999). *Tadpoles: The Biology of Anuran Larvae*. Chicago, Illnois, University of Chicago Press.

Miller, C. T., Yelon, D., Stainier, D. Y. & Kimmel, C. B. (2003). Two endothelin 1 effectors, hand2 and bapx1, pattern ventral pharyngeal cartilage and the jaw joint. *Development*, **130**, 1353–1365.

Naumann, B. & Olsson, L. (2018). Three-dimensional reconstruction of the cranial and anterior spinal nerves in early tadpoles of *Xenopus laevis* (Pipidae, Anura). *Journal of Comparative Neurology*, **526**, 836–857.

Newman, C. S., Grow, M.W., Cleaver, O., Chia, F. & Krieg, P. (1997). Xbap, a vertebrate gene related to bagpipe, is expressed in developing craniofacial structures and in anterior gut muscle. *Developmental Biology*, **181**, 223–33.

Newman, C. S. & Krieg, P. A. (1999). The *Xenopus* bagpipe-related homeobox gene zampogna is expressed in the pharyngeal endoderm and the visceral musculature of the midgut. *Development Genes and Evolution*, **209**, 132–134.

Nieuwkoop, P. & Faber, J. (1994). Normal Table of *Xenopus laevis* (Daudin). A Systematical and Chronological Survey of the Development from the Fertilized Egg Till the End of Metamorphosis). New York, Garland Publishing.

Olsson, L. & Hanken, J. (1996). Cranial neural-crest migration and chondrogenic fate in the oriental fire-bellied toad *Bombina orientalis*: defining the ancestral pattern of head development in anuran amphibians. *Journal of Morphology*, **229**, 105–120.

Pitsillides, A. A. & Ashhurst, D. E. (2008). A critical evaluation of specific aspects of joint development. *Developmental Dynamics*, 237, 2284–2294.

Riedelsheimer, B. & Büchl-Zimmermann, S. (2015). Färbungen, pp. 171–282 *in*: Mulisch, m. & Welsch, U. (eds), *Romeis - Mikroskopische Technik*. Berlin, Heidelberg, Springer.

Rinon, A., Lazar, S., Marshall, H., Büchmann-Møller, S., Neufeld, A., Elhanany-Tamir, H., Taketo, M.M., Sommer, L., Krumlauf, R. & Tzahor, E. (2007). Cranial neural crest cells regulate head muscle patterning and differentiation during vertebrate embryogenesis. *Development*, **134**, 3065–3075.

Rose, C. (2009). Generating, growing and transforming skeletal shape: insights from amphibian pharyngeal arch cartilages. *Bio Essays*, **31**, 287–299.

Rose, C. S. (2014). Caging, but not air deprivation, slows tadpole growth and development in the amphibian *Xenopus laevis*. *Journal of Experimental Zoology*, *Part A: Ecological Genetics and Physiology*, **321**, 365–375.

Rose, C. S., Murawinski, D. & Horne, V. (2015). Deconstructing cartilage shape and size into contributions from embryogenesis, metamorphosis, and tadpole and frog growth. *Journal of Anatomy*, **226**, 575–595.

De Sá, R. O. & Swart, C. C. (1999). Development of the suprarostral plate of pipoid frogs. *Journal of Morphology*, **240**, 143–153.

Sadaghiani, B. & Thiébaud, C. H. (1987). Neural crest development in the *Xenopus laevis* embryo, studied by interspecific transplantation and scanning electron microscopy. *Developmental Biology*, **124**, 91–110.

Schmidt, J., Schuff, m. & Olsson, L. (2011). A role for FoxN3 in the development of cranial cartilages and muscles in *Xenopus laevis* (Amphibia: Anura: Pipidae) with special emphasis on the novel rostral cartilages. *Journal of Anatomy*, **218**, 226–242.

Schuff, M., Rössner, A., Wacker, S. A., Donow, C., Gessert, S. & Knöchel W. (2007). FoxN3 is required for craniofacial and eye development of *Xenopus laevis*. *Developmental Dynamics*, **236**, 226–239.

Sokol, O. m. (1977). The free swimming *Pipa* larvae, with a review of pipid larvae and pipid phylogeny (Anura: Pipidae). *Journal of Morphology*, **154**, 357–425.

Square, T., Jandzik, D., Cattell, M., Coe, A., Doherty, J. & Medeiros, D. M. (2015). A gene expression map of the larval *Xenopus laevis* head reveals developmental changes underlying the evolution of new skeletal elements. *Developmental Biology*, **397**, 293–304.

SVENSSON, M. E. & HAAS, A. (2005). Evolutionary innovation in the vertebrate jaw: a derived morphology in anuran tadpoles and its possible developmental origin. *BioEssays*, **27**, 526–532.

TUCKER, A. S. (2004). Bapx1 regulates patterning in the middle ear: altered regulatory role in the transition from the proximal jaw during vertebrate evolution. *Development*, **131**, 1235–1245.

WILSON, J. & TUCKER, A. S. (2004). Fgf and Bmp signals repress the expression of Bapx1 in the mandibular mesenchyme and control the position of the developing jaw joint. *Developmental Biology*, **266**, 138–150.

WOLLENBERG VALERO, K. C., GARCIA-PORTA, J., RODRÍGUEZ, A., ARIAS, M., SHAH, A., RANDRIANIAINA, R.D., BROWN, J.L., GLAW, F., AMAT, F., KÜNZEL, S., METZLER, D., ISOKPEHI, R. D. & VENCES, M. (2017). Transcriptomic and macroevolutionary evidence for phenotypic uncoupling between frog life history phases. *Nature Communications*, **8**, 15213.

YAMASHITA, S., ANDOH, M., UENO-KUDOH, H., SATO, T., MIYAKI, S. & ASAHARA, H. (2009). Sox9 directly promotes Bapx1 gene expression to repress Runx2 in chondrocytes. *Experimental Cell Research*, **315**, 2231–2240.

ZIERMANN, J. M. & OLSSON, L. (2007). Patterns of spatial and temporal cranial muscle development in the African clawed frog, *Xenopus laevis* (Anura: Pipidae). *Journal of Morphology*, **268**, 791–804.

Supplement I

List of specimens examined

Species	Preparation	number of larvae	stage
Xenopus laevis (Daudin, 1802)	Zax-MO1 experiments	540	various
	Zax-MO1 controls	90	„
	Zax-MO2 experiments	180	„
	Zax-MO2 controls	90	„
	Co-MO	90	„
	needle penetration	90	„
	qPCR	27 treated	NF1-45
		27 untreated	NF1-45
	histology	42 treated	NF40-46
		29 untreated	NF35-48
	antibody-staining	37 treated	NF40-46
		14 untreated	NF35-48
Hymenochirus boettgeri (Tornier, 1896)	antibody-staining	3	Go25